

Self-Phase Modulation Compensation in a Regenerative Amplifier Using Cascaded Second-Order Nonlinearities

Laser systems delivering short optical pulses are commonly built using chirped-pulse amplification (CPA).¹ CPA decreases the intensity of the pulse being amplified below the damage threshold of optical components and reduces the accumulated intensity-dependent nonlinearity. With or without CPA, an optical pulse propagating in a laser system can accumulate significant amounts of phase via self-phase modulation (SPM), i.e., a phase $\varphi(\vec{r}, t) = \Gamma I(\vec{r}, t)$, at intensities well below the damage threshold. SPM is a concern because it leads to spatial self-focusing and spectral broadening that can disrupt the amplification process. CPA is often space consuming because of the footprint of grating-based stretchers and compressors. It is difficult to implement on low-bandwidth pulses because of the large dispersion required to significantly stretch these pulses. SPM compensation methods are attractive for amplifying picosecond pulses at intensities below the damage threshold without CPA.

In fiber-based systems² temporal phase modulators can be used to compensate for SPM, but this compensation is limited to particular operating conditions. For a pulse propagating in free space, a phase that is negatively proportional to the intensity can be induced by propagation at a specific wavelength in a semiconductor wafer^{3,4} or in a cesium vapor,⁵ but these processes have limited wavelength and nonlinearity tunability. Cascaded nonlinearities obtained by propagation in a nonlinear crystal detuned from phase matching introduce an intensity-

dependent phase.⁶ SPM compensation using a cascaded nonlinearity with a negative n_2 is simple to implement, relies on commercially available nonlinear crystals that can be procured with high quality, has a small footprint, is usable at a wide range of optical wavelengths, and provides nonlinearity tunability. The accumulated intensity-dependent phase is a linear function of the intensity only up to ~ 1 rad. This compensation strategy is not suitable for large, accumulated nonlinear phase shifts, but it is well suited for iterative compensation of the small nonlinear phase shifts from multiple passes in a regenerative amplifier cavity, even if these phase shifts add up to a large phase shift in the absence of compensation. Intracavity nonlinearity compensation has been used to compensate for the pump-pulse time-dependent phase shift that decreases the enhancement factor of a cavity-enhanced optical parametric chirped-pulse-amplification system;⁷ to control low-power continuous-wave light via optical bistability;⁸ and to mode-lock a continuous-wave (cw)-pumped laser;⁹ however, it has not been studied or demonstrated to control the properties of a pulse amplified by a laser amplifier.

Simulations have been conducted to understand the origin of SPM in the Nd:YLF regenerative amplifier schematized in Fig. 137.74. This regenerative amplifier architecture is used to amplify nanosecond pulses at 1053 nm suitable to seed large-scale Nd:glass laser systems¹⁰ and for amplification with pulse durations limited by gain narrowing in the Nd:YLF (~ 12 ps),

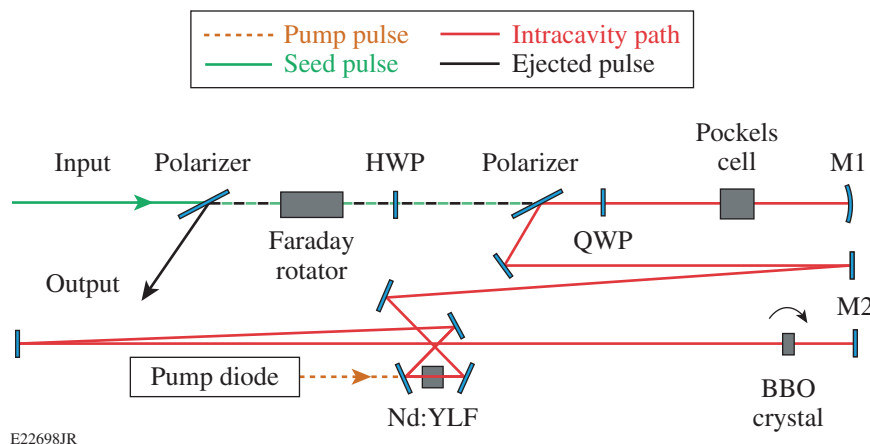


Figure 137.74
Regenerative amplifier layout. HWP = half-wave plate; QWP = quarter-wave plate; BBO: beta-barium borate.

E22698JR

e.g., to generate short UV pulses after fourth-harmonic generation¹¹ and optical-parametric-amplifier pump pulses after second-harmonic generation (SHG).¹² The amplifier has a near-hemispherical cavity with an end-cavity plane mirror and an end-cavity spherical mirror ($R = 5$ m). The propagation simulations in the paraxial approximation are implemented with *MATLAB*¹³ in cylindrical coordinates, i.e., the field is a function of the radius r and time t . Nonlinearity in the deuterated potassium dihydrogen phosphate (DKDP) Pockels cell (PC), the Nd:YLF crystal, air, and the Faraday isolator is taken into account. The PC is the largest SPM contributor. An intracavity pulse train measured behind one of the cavity mirrors is used to scale the pulse energy after each pass in the Nd:YLF crystal. The simulations show that the amplified pulse accumulates temporal phase (leading to spectral broadening) but no spatial phase (which could lead to self-focusing). The intracavity spectral broadening is uniform across the beam at the output of the regenerative amplifier but is slightly spatially varying after the isolator. The uniform intracavity spectral broadening and absence of a significant spatially varying wavefront are explained by the large number of passes in the cavity that constrain the spatial phase at the two end mirrors and constrain the beam to the highest-gain cavity eigenmode.

Without SPM compensation, amplification to 0.5 mJ after 124 round-trips leads to ~ 1.8 rad of accumulated phase, including ~ 1.1 rad from propagation in the intracavity PC and ~ 0.4 rad from the extracavity Faraday isolator. The intracavity beam remains approximately Gaussian with a flat spatial phase at mirror M2, but the waist size decreases by $\sim 5\%$ when the intracavity energy reaches 0.5 mJ. Propagation in the PC at the last pass induces a nonlinear phase smaller than 0.1 rad. In this regime, the spatiotemporal phase induced by the cascaded nonlinearity is proportional to the intensity for an adequately detuned crystal. Simulations show that a compensating element with nonlinear coefficient $\Gamma = -3 \times 10^{-15}$ m²/W located close to mirror M2 provides minimal spectral broadening at output energies up to ~ 2 mJ (Fig. 137.75). The polarization at M2 is linear for all passes, as required for the operation of the cascaded nonlinearities, and this location is convenient to access. Compensation closer to the PC—the main contributor to intracavity nonlinearity—operates over a larger range of energies, but it was not experimentally attempted because of layout issues.

When a nonlinear crystal (nonlinear coefficient d_{eff} and refractive indices n_{ω} and $n_{2\omega}$ at the fundamental frequency ω and upconverted frequency 2ω) is significantly detuned out of phase matching ($\Delta k(\Delta kL \gg 1)$), cascaded nonlinearities lead

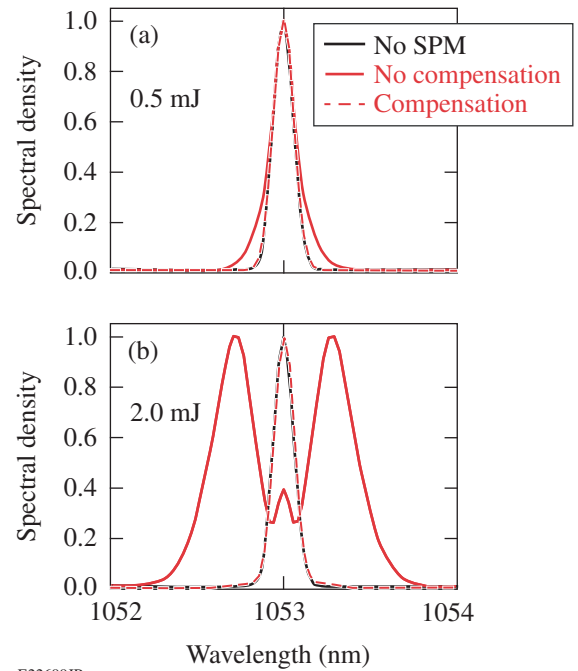


Figure 137.75

Simulated optical spectra without self-phase modulation (SPM) in the cavity (black line), with SPM and no compensation (solid red line), and with SPM and compensation (dashed red line) at output energies of (a) 0.5 mJ and (b) 2.0 mJ.

to an effective nonlinear index on the field at the fundamental wavelength λ (Ref. 6) given by

$$n_2^{\text{eff}} = -\frac{4\pi d_{\text{eff}}^2}{c\epsilon_0 \lambda n_{2\omega} n_{\omega}^2 \Delta k}. \quad (1)$$

Operating at large Δk allows one to precisely tune the nonlinearity by tuning the phase-matching angle. A 5-mm beta-barium–borate (BBO) crystal antireflection coated at 1053 nm and 526.5 nm was placed in the cavity close to mirror M2, with phase matching around a vertical axis.

Experimental results were obtained on two regenerative amplifiers seen in the layout in Fig. 137.74. These systems amplify the pump pulse for the optical parametric amplifier in the front end of the Multi-Terawatt Laser Facility^{12,14} and in the ultra-broadband front end.¹⁵ They are both seeded by ~ 6 -nm optical pulses centered at 1053 nm originating from mode-locked lasers. The output energy decreased by $\sim 15\%$ when the compensation crystal was introduced, most likely because of reflection losses. The optimal SPM compensation was determined by measuring the output spectrum after the Faraday isolator for various detuning angles. The narrowest spectrum

has a full width at half maximum (FWHM) equal to 0.14 nm and is similar to the fluorescence spectrum of the unseeded amplifier. Figure 137.76 shows the optical spectra measured at output energies of ~ 0.5 mJ and ~ 0.8 mJ without and with nonlinearity compensation. Operation at higher energy was obtained by increasing the pump-diode current and decreasing the number of round-trips in the cavity to eject the pulse at the peak of the buildup. Very good SPM compensation was obtained at the higher energy without retuning the intracavity BBO crystal. SPM compensation was performed on a second regenerative amplifier that operated with a larger number of round-trips at an output energy of 0.8 mJ. Excellent compensation of the larger spectral broadening was also obtained.

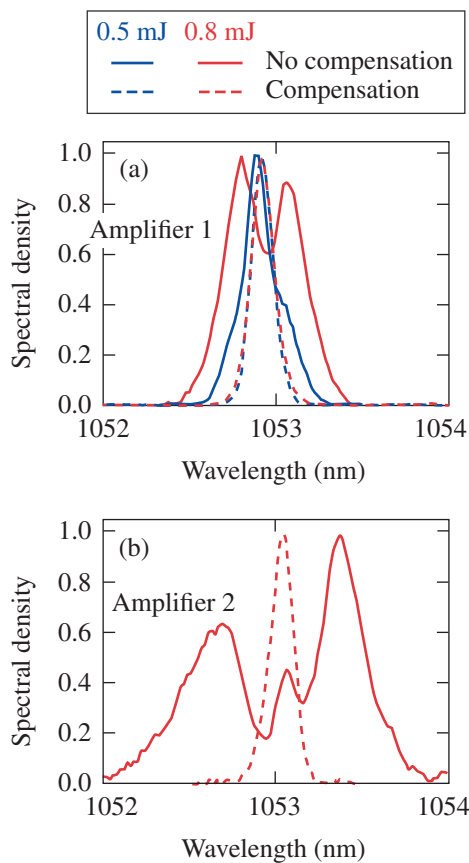


Figure 137.76 Optical spectra without compensation (solid lines) and with compensation (dashed line) for output energies of 0.5 mJ and 0.8 mJ, respectively. The data were measured on two different regenerative amplifiers.

Optimal compensation was obtained for these two amplifiers when the internal angular detuning was $\sim 0.9^\circ$ from phase matching ($\Delta kL \sim 90$), corresponding to a nonlinear index -1.7×10^{-15} cm²/W and nonlinearity $\Gamma = -5.1 \times 10^{-15}$ m²/W. The

magnitude of the nonlinearity is larger than what has been identified by simulations, but the Kerr nonlinearity of the intracavity BBO crystal ($n_2 = 5 \times 10^{-16}$ cm²/W) (Ref. 16) reduces the compensating nonlinearity by $\sim 30\%$. The simulations ignore propagation in various short optical components such as wave plates and polarizers. Considering the uncertainties on the nonlinear index of DKDP and BBO,^{16,17} the detuning experimentally required for SPM compensation is in good agreement with expectations.

The output energy at 1053 nm and intracavity-generated energy at 526.5 nm were characterized when finely tuning the compensating crystal. The SHG energy was measured behind the end mirror M2 (transmission $\sim 85\%$ at 526.5 nm) and was not temporally resolved, i.e., the reported value corresponds to the total SHG energy reaching the energy meter during amplification for all round-trips. Anticorrelated variations of these energies are observed (Fig. 137.77) because intracavity SHG is a loss mechanism for the pulse being amplified. The period of these variations is consistent with phase matching in a 5-mm BBO crystal, where the efficiency of the SHG process is proportional to $[\text{sinc}(\Delta kL/2)]^2$. Because of the $\sim 10\%$ variation of the output energy, the crystal detuning angle must be controlled to $\sim 0.01^\circ$ to maximize the output energy.

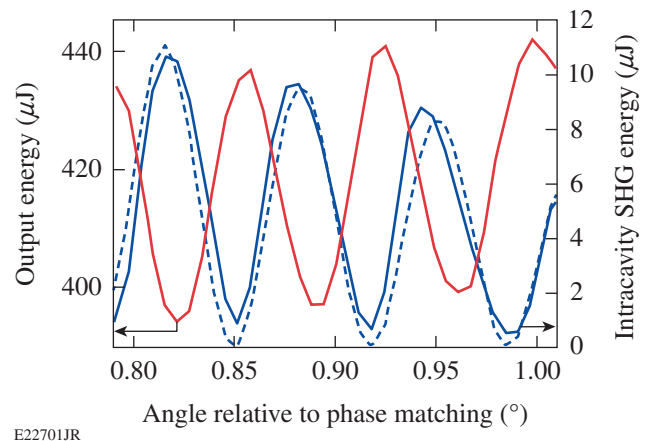
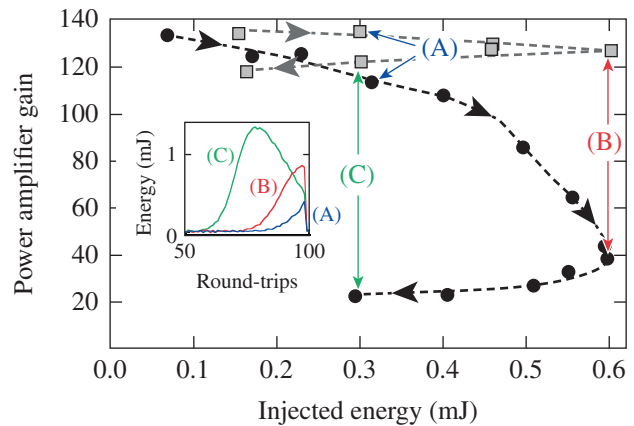


Figure 137.77 Regenerative amplifier output energy (red line) and intracavity second-harmonic-regeneration (SHG) energy generated in the BBO crystal leaking through mirror M2 (solid blue line) compared to arbitrarily scaled SHG efficiency $[\text{sinc}(\Delta kL/2)]^2$ (dashed blue line).

Another experiment was performed to highlight the advantage of SPM compensation in a laser system composed of multiple amplifiers based on the same laser material. The highest efficiency for an amplifier, particularly in the unsaturated regime, is obtained when the amplifier gain is high over the

entire spectral density of the seed pulse. Without compensation, SPM in the regenerative amplifier broadens the spectrum of the pulse seeded in a custom-built flash-lamp-pumped power amplifier based on three Nd:YLF rods (total length = 265 mm). For this experiment, the regenerative amplifier output pulse energy was throttled down by 25% independently of the energy, to avoid damage at high energy; e.g., the input energy to the power amplifier is 0.6 mJ at the nominal regenerative-amplifier energy of 0.8 mJ. The power amplifier's spectral gain was not measured, but by comparing its small signal gain to the gain of the regenerative amplifier [$\sim 10^2$ and $\sim 10^8 = (10^2)^4$, respectively], we estimated its FWHM to be twice the FWHM of the regenerative-amplifier gain; i.e., 0.28 nm, assuming Gaussian gain functions. This FWHM was significantly smaller than the width of the optical spectra observed in the absence of SPM compensation.

The regenerative amplifier's pump-diode current was scanned to vary the accumulated intracavity nonlinearity of the output pulse and the energy injected into the power amplifier without modifying the ejection timing (examples shown in the inset of Fig. 137.78). Nominal operation corresponds to ejection at the peak of the intracavity buildup [(B) in Fig. 137.78]. Under the simplifying assumption that the accumulated nonlinear phase is proportional to the sum of the energy of all the pulses in the measured pulse train, the low-current and high-current configurations [(A) and (C) in Fig. 137.78] correspond to 32% and 308%, respectively, of the nominal nonlinear phase for the same injected energy of 0.3 mJ. The power-amplifier gain for a small amount of SPM is ~ 135 . Without compensation, the gain decreases steadily when the regenerative amplifier's intracavity nonlinearity increases, reaching ~ 40 at the maximal regenerative amplifier output energy [pumping condition (B)] and ~ 20 for higher intracavity nonlinearity [pumping condition (C)]. Without compensation, the highest output energy, ~ 40 mJ, is obtained when the injected energy is ~ 0.4 mJ. Large spectral broadening of the regenerative amplifier's output pulse was observed as the current was increased because of intracavity SPM. When the latter was compensated without retuning the cascaded nonlinearity, the regenerative amplifier's pump-current increase did not induce a significant decrease in the power amplifier's efficiency. In particular, the energy gain remained higher than 120 in the three pumping conditions shown in Fig. 137.78. The highest output energy, ~ 75 mJ, was obtained for the highest injected energy, 0.6 mJ, demonstrating a gain of 125. These experimental results confirm that intracavity SPM compensation is suitable for SPM compensation over a large range of operating conditions, making efficient amplification possible in later amplification stages.



E22702JR

Figure 137.78

Power-amplifier gain versus injected energy without (solid black circles) and with (solid gray squares) SPM compensation in the regenerative amplifier. Examples of regenerative-amplifier buildup pulse train envelopes are shown in the inset: (A), (B), and (C) correspond to regenerative-amplifier output energies of 0.4 mJ, 0.8 mJ, and 0.4 mJ, respectively; i.e., injected energies of 0.3 mJ, 0.6 mJ, and 0.3 mJ after throttling down by 25%.

Intracavity nonlinearity compensation in a regenerative amplifier has been studied via simulations and experiments in the context of short-pulse amplification in Nd:YLF. DKDP Pockels-cell Kerr nonlinearity is the main contributor to the overall nonlinearity. Self-phase modulation leads mostly to spectral broadening because the large number of round-trips in the cavity constrains the beam profile to the spatial mode of the cavity having the smallest overall losses. Intracavity compensation of SPM with cascaded nonlinearities is a powerful strategy to compensate for the small nonlinear phase shifts accumulated in optical components at each round-trip. Experimental results obtained with a BBO crystal in two Nd:YLF regenerative amplifiers confirm the validity of this approach. Significant reduction of spectral broadening allows for high-efficiency amplification of the generated pulses in two Nd:YLF power amplifier.

This work can be extended in different directions: First, it is interesting to theoretically and experimentally test the limit of this approach, e.g., in terms of per-round-trip nonlinear phase shift and relative location of elements inducing nonlinearities. Applications to amplifiers with broader spectral gain capable of generating subpicosecond pulses are of practical interest, following the demonstration that cascaded nonlinearities can be used at these shorter pulse durations.¹⁸ Cascaded nonlinearities can be precisely tuned to increase the spectral content of the amplified optical pulse and allow for pulse recompression, as demonstrated with intracavity nonlinear propagation in a Nd:glass amplifier,¹⁹ or seeding of another amplifier with gain centered at a different wavelength.

ACKNOWLEDGMENT

This material is based upon work supported by the Department of Energy National Nuclear Security Administration under Award Number DE-NA0001944, the University of Rochester, and the New York State Energy Research and Development Authority. The support of DOE does not constitute an endorsement by DOE of the views expressed in this article.

REFERENCES

1. D. Strickland and G. Mourou, *Opt. Commun.* **56**, 219 (1985).
2. J. van Howe, G. Zhu, and C. Xu, *Opt. Lett.* **31**, 1756 (2006).
3. M. Sheik-Bahae *et al.*, *IEEE J. Quantum Electron.* **27**, 1296 (1991).
4. O. A. Konoplev and D. D. Meyerhofer, *IEEE J. Sel. Top. Quantum Electron.* **4**, 459 (1998).
5. R. H. Lehberg, J. Reintjes, and R. C. Eckardt, *Appl. Phys. Lett.* **30**, 487 (1977).
6. G. I. Stegeman, D. J. Hagan, and L. Torner, *Opt. Quantum Electron.* **28**, 1691 (1996).
7. F. Ö. Ilday and F. X. Kärtner, *Opt. Lett.* **31**, 637 (2006).
8. A. G. White, J. Mlynek, and S. Schiller, *Europhys. Lett.* **35**, 425 (1996).
9. M. Zavelani-Rossi, G. Cerullo, and V. Magni, *IEEE J. Quantum Electron.* **34**, 61 (1998).
10. A. V. Okishev and J. D. Zuegel, *Appl. Opt.* **43**, 6180 (2004).
11. C. Dorrer, I. A. Begishev, A. V. Okishev, and J. D. Zuegel, *Opt. Lett.* **32**, 2143 (2007).
12. D. H. Froula, R. Boni, M. Bedzyk, R. S. Craxton, F. Ehrne, S. Ivancic, R. Jungquist, M. J. Shoup, W. Theobald, D. Weiner, N. L. Kugland, and M. C. Rushford, *Rev. Sci. Instrum.* **83**, 10E523 (2012).
13. MATLAB® The MathWorks, Inc., Natick, MA 01760-2098 (<http://www.mathworks.com>).
14. V. Bagnoud, I. A. Begishev, M. J. Guardalben, J. Puth, and J. D. Zuegel, *Opt. Lett.* **30**, 1843 (2005).
15. J. Bromage, C. Dorrer, M. Millicchia, J. Bunkenburg, R. Jungquist, and J. D. Zuegel, in *Conference on Lasers and Electro-Optics 2012*, OSA Technical Digest (online) (Optical Society of America, 2012), Paper CTh1N.7.
16. M. Bache *et al.*, *Opt. Mater. Express* **3**, 357 (2013).
17. I. A. Kulagin *et al.*, *J. Opt. Soc. Am. B* **23**, 75 (2006).
18. F. Wise, L. Qian, and X. Liu, *J. Nonlinear Opt. Phys. Mater.* **11**, 317 (2002).
19. L. Yan, Y.-Q. Liu, and C. H. Lee, *IEEE J. Quantum Electron.* **39**, 2194 (1994).

